

## In vivo measurement of the myelin g-ratio with histological validation

Nikola Stikov<sup>1</sup>, Jennifer S.W. Campbell<sup>1</sup>, Mariette Lavallée<sup>1</sup>, Thomas Stroh<sup>1</sup>, Stephen Frey<sup>1</sup>, Jennifer Novek<sup>1</sup>, Stephen Nuara<sup>1</sup>, Ming-Kai Ho<sup>1</sup>, Barry Bedell<sup>1</sup>, and G. Bruce Pike<sup>1,2</sup>

<sup>1</sup>Montreal Neurological Institute, McGill University, Montreal, QC, Canada, <sup>2</sup>Hotchkiss Brain Institute, University of Calgary, Calgary, AB, Canada

**TARGET AUDIENCE:** Researchers studying myelination, brain microstructure, and the relationship between diffusion and magnetization transfer.

**PURPOSE:** The myelin g-ratio, defined as the ratio between the inner and the outer diameter of the myelin sheath, is a fundamental property of white matter<sup>1,2</sup> that can be computed from a simple formula (Fig. 1) relating the myelin volume fraction (MVF) to the fiber volume fraction (FVF) or the axon volume fraction (AVF)<sup>3</sup>. Recent studies have suggested that the sexual dimorphism in white matter development is due to a higher g-ratio (relatively thinner myelin) in adolescent boys<sup>4</sup>. Additionally, *in vivo* imaging of the myelin thickness in multiple sclerosis could provide a real-time tool for tracking myelination in lesions, facilitating the development and evaluation of new therapeutic agents that promote remyelination. In this abstract, a unique combination of magnetization transfer, diffusion imaging and histology is presented, providing a novel method for validating the *in vivo* measurements of the myelin g-ratio.

**METHODS:** MRI measurements were performed in the corpus callosum (CC) of one cynomolgus (long-tailed) macaque, using a custom 6-channel head coil in a 3T Siemens Trio MRI scanner. The slice thickness for all MRI protocols was chosen to span the width of the macaque corpus callosum (3mm), resulting in anisotropic voxels (.7 x .7 x 3mm<sup>3</sup>) with higher resolution in the sagittal plane. MVF was computed from the fractional pool size F, using an in-house quantitative magnetization transfer (qMT) protocol consisting of variable flip angle T1 mapping<sup>5</sup>, actual flip angle imaging (AFI) B1 mapping<sup>6</sup>, 10-point uniform sampling of the z-spectrum<sup>7</sup>, and 8 signal averages. The coefficient of proportionality relating F to MVF was computed from a linear regression to the histology data. AVF was computed from the anisotropically restricted signal fraction, obtained using a two-shell NODDI protocol<sup>8</sup>. While diffusion is highly restricted within the myelin bilayers, the signal from myelin is very small for this diffusion acquisition, hence the myelin contribution to the restricted signal fraction was considered negligible for the purpose of estimating AVF. The MVF, however, is significant, meaning the true axon volume fraction from NODDI is given by AVF = (1 - MVF)(1 - v<sub>iso</sub>)v<sub>ic</sub>, with v<sub>iso</sub> and v<sub>ic</sub> as described by Zhang et al.<sup>8</sup> Five signal averages of 100 diffusion encoding directions with b=1000 s/mm<sup>2</sup> and b=2450 s/mm<sup>2</sup>, as well as two b=0 s/mm<sup>2</sup> images were acquired using a 2D TRBE<sup>9</sup> single shot SE-EPI sequence with sagittal slices. After the scan, the macaque was perfused at euthanasia with 2% glutaraldehyde and 2% PFA. The corpus callosum was extracted and divided into eight segments from anterior to posterior, and electron microscopy was performed on three samples from each of the segments 1-8 at 1900X magnification. The EM images (Fig. 3) were classified into axon (blue) and myelin (red), and the AVF, MVF, and g-ratio were computed from the histology. For the MRI measurements, the CC was skeletonized and divided into 8 ROIs. For each ROI the signal was averaged before fitting for AVF, MVF, and the g-ratio.

**RESULTS:** Figure 2 shows the computed AVF, MVF, and g-ratio maps in the CC. Figure 3 shows the comparison between MRI and histology in the CC. The g-ratio Pearson correlation coefficient between MRI and histology was r = .83, with p = .011.

**DISCUSSION:** The trends in the qMRI measurements are consistent with literature. In particular, the AVF exhibits a high-low-high trend in the CC, which has been reported previously<sup>2,9</sup>, and the g-ratio is higher in the super-axons found in the splenium<sup>10</sup>. Also, Fig. 3 shows that compared to AVF and MVF, the g-ratio has a narrower dynamic range and smaller standard errors of the mean. This is consistent with the literature claims that the g-ratio is expected to be relatively constant, even if the AVF and MVF vary<sup>1,2,11</sup>. MRI was performed on a much coarser scale than histology, so it is important to note that the MRI values are averages over a region that might have microscopic heterogeneity. Yet, our mean MRI values are very close to the mean histological measurements, and the g-ratio computed from MRI exhibits a high correlation with histology. In conclusion, diffusion and magnetization transfer provide complementary measurements, which can be combined to estimate the myelin g-ratio *in vivo*.

**REFERENCES:** [1] Rushton, W., J Physiol 1951. [2] Chomiak and Hu. PLoS ONE 2009. [3] Stikov et al. Neuroimage 2011. [4] Paus and Toro, Front Neuroanat 2009. [5] Fram et al. Magnetic Resonance Imaging 1987. [6] Yarnykh et al. MRM 2007. [7] Levesque et al. MRM 2011. [8] Zhang et al. NeuroImage 2012. [9] Reese et al. MRM 2003. [10] Lamantia and Rakic. J. Comp. Neurology 1990. [11] Pajevic et al. PLoS ONE 2013.

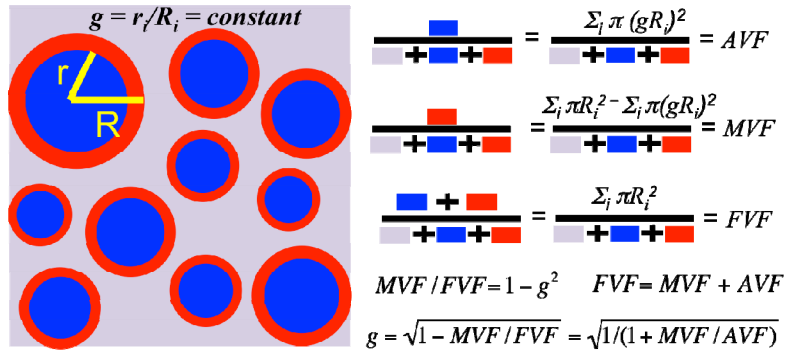


Figure 1: White matter model defining the g-ratio, AVF, MVF, and FVF

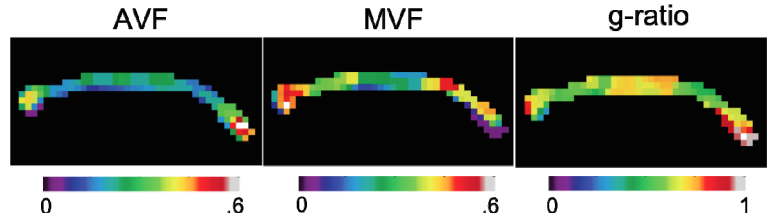


Figure 2: MVF, AVF, and g-ratio maps (median-filtered) in the macaque corpus callosum

AVF	.42	.36	.38	.35	.30	.38	.27	.71
MVF	.40	.40	.47	.29	.34	.35	.58	.28
g-ratio	.72	.69	.67	.74	.69	.72	.57	.85
Imaging								
Histology	Genu (1)	(2)	(3)	(4)	(5)	(6)	(7)	Splenium (8)
AVF	.36 (.02)	.33 (.04)	.25 (.03)	.33 (.02)	.39 (.03)	.31 (.02)	.25 (.01)	.37 (.04)
MVF	.40 (.05)	.38 (.02)	.35 (.02)	.36 (.03)	.37 (.02)	.44 (.02)	.43 (.03)	.29 (.03)
g-ratio	.69 (.03)	.69 (.03)	.64 (.04)	.69 (.02)	.72 (.02)	.64 (.01)	.60 (.02)	.74 (.04)

Figure 3: Segmented electron micrographs for eight macaque corpus callosum segments showing myelin (red) and axons (blue). MRI (top) and histological (bottom) measurements for AVF, MVF, and g-ratio, with standard error of the mean in parenthesis.